

基于决策树的海底隧道围岩抗渗性分级方法

郑岚翔，张顶立，孙振宇

ANTI-SEEPAGE CLASSIFICATION OF SURROUNDING ROCK FOR SUBSEA TUNNELS BASED ON DECISION TREE

Zheng Lanxiang, Zhang Dingli, and Sun Zhenyu

在线阅读 View online: <https://doi.org/10.6052/0459-1879-24-408>

您可能感兴趣的其他文章

Articles you may be interested in

考虑渗流效应的深埋海底隧道围岩与衬砌结构应力场研究

RESEARCH ON STRESS FIELD OF SURROUNDING ROCK AND LINING STRUCTURE OF DEEP-BURIED SUBSEA TUNNEL CONSIDERING SEEPAGE EFFECT

力学学报. 2022, 54(5): 1322–1330

浅埋海底隧道围岩应力复势函数显式解

EXPLICIT SOLUTION OF STRESS COMPLEX POTENTIAL FUNCTION FOR SURROUNDING ROCK OF SHALLOW SUBSEA TUNNEL

力学学报. 2023, 55(7): 1505–1516

深埋三连拱隧道围岩压力计算方法

CALCULATION METHOD FOR SURROUNDING ROCK PRESSURE OF DEEPLY BURIED TRIPLE-ARCH TUNNEL

力学学报. 2024, 56(11): 3213–3226

水平互层围岩隧道破坏机理及其范围预测模型

FAILURE MECHANISM AND SCOPE PREDICTION MODEL OF HORIZONTAL INTERBEDDED SURROUNDING ROCK TUNNEL

力学学报. 2022, 54(10): 2835–2849

流变岩体中让压支护作用下隧道力学行为研究

INVESTIGATION ON THE MECHANICAL BEHAVIOR OF TUNNEL SUPPORTED BY YIELDING SUPPORTS IN RHEOLOGICAL ROCKS

力学学报. 2020, 52(3): 890–900

考虑锚杆作用的深埋软岩隧道黏弹塑性力学响应解析

ANALYTICAL APPROACH TO THE VISCOELASTO-PLASTIC MECHANICAL RESPONSE OF DEEP SOFT ROCK TUNNEL CONSIDERING THE ROCKBOLT REINFORCEMENT EFFECT

力学学报. 2022, 54(2): 445–458



关注微信公众号，获得更多资讯信息

基于决策树的海底隧道围岩抗渗性分级方法¹⁾

郑岚翔 张顶立 孙振宇²⁾

(北京交通大学城市地下工程教育部重点实验室, 北京 100044)

摘要 在进行海底隧道防排水系统设计时, 为了实现排水量的主动控制, 需对围岩自身堵水能力有清楚认识。首先提出围岩抗渗性的概念, 即隧道围岩抵抗水流渗透的能力, 推导了裂隙岩体非线性渗流条件下隧道原始渗水量预测公式, 揭示了工程地质条件、水力联系和隧道尺寸效应等因素对围岩抗渗性的影响机理; 在此基础上, 通过对 52 个典型海底及富水隧道断面的渗水案例数据的统计分析, 明确提出了隧道围岩抗渗性影响因素为岩石覆盖层厚度、水头高度、岩石单轴饱和抗压强度以及体积节理数, 为指标建立了围岩抗渗性分级标准。利用二分法及训练数据集的信息增益率对统计数据进行机器学习, 建立了可分析连续值属性的决策树模型, 由此可通过该模型对围岩参数进行搜索以实现围岩抗渗性分级。最后将该模型应用于胶州湾第二海底隧道海域钻爆段, 验证了本文抗渗性分级方法的合理性和可行性。文章研究成果为海底隧道排水量控制标准的确定提供了理论依据, 相较于传统的围岩分级方法, 抗渗性分级综合考虑了围岩条件及其渗流力学响应, 据此采取的防排水设计与分区防水方案将更为科学合理。

关键词 隧道工程, 海底隧道, 抗渗性分级, 统计分析, 决策树模型

中图分类号: U459.5 文献标识码: A

DOI: [10.6052/0459-1879-24-408](https://doi.org/10.6052/0459-1879-24-408) CSTR: [32045.14.0459-1879-24-408](https://cstr.zjlab.org.cn/cstr/32045.14.0459-1879-24-408)

ANTI-SEEPAGE CLASSIFICATION OF SURROUNDING ROCK FOR SUBSEA TUNNELS BASED ON DECISION TREE¹⁾

Zheng Lanxiang Zhang Dingli Sun Zhenyu²⁾

(Key Laboratory for Urban Underground Engineering of Ministry of Education, Beijing Jiaotong University, Beijing 100044, China)

Abstract When designing the waterproofing and drainage system for an subsea tunnel, it is crucial to have a clear understanding of the surrounding rock's inherent water-blocking capabilities to achieve active control over the drainage volume. This paper first introduces the concept of the surrounding rock impermeability, defined as the ability of the rock's ability to resist water infiltration into the tunnel. A predictive formula for water inflow is derived, taking into account nonlinear seepage conditions in fractured rock masses. The formula considers several factors that influence impermeability, including engineering geological conditions, hydraulic connectivity within the rock, and the size of the tunnel. On this basis, the study performs a statistical analysis of water inflow data from 52 typical subsea tunnel sections, particularly those in water-rich environments, to identify key factors influencing the impermeability of surrounding rock. These factors include rock cover thickness, hydraulic head, uniaxial saturated compressive strength of the rock, and

2024-08-27 收稿, 2025-01-09 录用, 2025-01-09 网络版发表。

1) 中央高校基本科研业务费专项资金(2022JBZY041)和国家自然科学基金(52208382)资助项目。

2) 通讯作者: 孙振宇, 副教授, 主要研究方向为隧道与地下工程. E-mail: Zhenyus@bjtu.edu.cn

引用格式: 郑岚翔, 张顶立, 孙振宇. 基于决策树的海底隧道围岩抗渗性分级方法. 力学学报, 2025, 57(2): 488-501

Zheng Lanxiang, Zhang Dingli, Sun Zhenyu. Anti-seepage classification of surrounding rock for subsea tunnels based on decision tree. Chinese Journal of Theoretical and Applied Mechanics, 2025, 57(2): 488-501

volumetric joint count. These factors are used as indicators to establish a classification standard for the rock impermeability. To enhance the classification process, machine learning techniques are employed. The bisection method and information gain ratio from the training dataset are used to analyze the data. A decision tree model capable of handling continuous-valued attributes is established. This model allows for the classification of surrounding rock impermeability based on the relevant rock parameters, thus enabling a more automated and data-driven approach to impermeability classification. Finally, the model is applied to the drill-and-blast section of the Qingdao-Jiaozhou Bay Second Subsea Tunnel, verifying the rationality and feasibility of the proposed anti-seepage classification method. The research findings provide a theoretical basis for determining drainage control standards in subsea tunnels. Compared to traditional rock mass classification methods, the anti-seepage classification method comprehensively considers the conditions of the surrounding rock and its seepage mechanical response, leading to a more scientific and reasonable approach to waterproofing design and zoned drainage strategies.

Key words tunnelling engineering, subsea tunnels, anti-seepage classification, statistical analysis, decision tree model

引言

海底隧道因采用 V 型纵坡导致渗水无法自然排出, 因此防排水问题是其建设与运营安全的重难点。纵观国内外水下隧道, 采用的防排水方式可分为全封堵式和排导式两种, 且都以二次衬砌作为主承载结构。全封堵式隧道衬砌承受的水压与地下水水头相当, 不适用于上覆水层高且埋深大的隧道工程。排导式防排水体系可一定程度上减小作用于衬砌结构上的外水压力, 并大大降低其劣化渗漏的几率, 使得衬砌结构经济合理。王梦恕等^[1]针对海底隧道提出了“堵水限排”的防水体系, 在考虑围岩加固圈稳定性的同时控制排水量。然而, 围岩加固圈及初支结构堵水的同时也承担了相应的水载荷, 需要综合考虑防排水系统的安全性与经济性。为了实现海底隧道“堵水限排”防排水系统的整体安全, 张顶立等^[2]提出构建主动控制式防排水系统, 其核心特色在于允许排水量的主动确定和堵水系统的协同设计。

防排水系统受围岩条件和水文地质条件等因素综合影响, 而其设计方案的主要区别在于对围岩堵水能力的认识以及允许排水量的确定^[3-5]。尽管目前国内外学者对海底隧道防排水设计理论及技术进行了大量研究^[6-15], 但对海底隧道的允许排水量并没有统一标准。日本青函海底隧道根据泵站抽水能力及二次衬砌承受水载荷的能力, 确定允许排水量为 $0.2736 \text{ m}^3/(\text{d}\cdot\text{m})$ ^[16-17], 挪威海底隧道考虑排水设备能力及经济性, 确定允许渗水量为 $0.432 \text{ m}^3/(\text{d}\cdot\text{m})$, 厦门翔安海底隧道海域强风化槽段设计排水量为 $2.5 \text{ m}^3/(\text{d}\cdot\text{m})$ ^[18], 戴鑫等^[19]通过对国内外已建成海底

隧道排水量调研分析, 结合具体工程情况确定珠江口铁路隧道矿山段排水量标准为 $0.3 \text{ m}^3/(\text{d}\cdot\text{m})$, 王秀英等^[20]采用数值模拟计算得到厦门海底隧道软弱围岩段限量排放后的渗水量为 $0.123 \text{ m}^3/(\text{d}\cdot\text{m})$ 。自 1965 年第一条水下隧道——打浦路隧道修建^[21], 我国水下隧道已发展近 60 年, 然而隧道允许排水量的确定仍主要依靠工程经验类比取值, 尚未形成可供参考的统一规范, 究其根本原因在于对围岩堵水能力认识不足, 使得防排水设计缺乏理论依据。

此外, 对于长大海底隧道而言, 常需采用分区防水设计, 而目前工程中该设计往往依赖于围岩分级的结果。事实上, 由于海底隧道所处的水文地质条件复杂, 与水的连通性存在差异性, 要想主动确定隧道允许排水量并给出防排水系统设计方法, 需对海底隧道围岩的堵水能力进行判断, 并据此制定不同的排水量控制标准。

本文提出隧道围岩抗渗性的概念, 推导非线性渗流条件下隧道原岩渗水量预测公式, 并结合海底隧道及富水隧道的大量现场实测数据, 确定抗渗性分级的评价指标, 建立围岩抗渗性分级标准, 采用机器学习的方法对海底隧道围岩抗渗性进行分级预测。由此可为海底隧道防排水系统的协同设计提供理论依据, 对于富水隧道的防排水设计也具有一定的借鉴意义。

1 围岩渗水量预测与抗渗性分析

1.1 围岩抗渗性定义

围岩抗渗性是指隧道围岩抵抗水流渗透的能

力, 其倒数即为在一定水压作用下引起的渗水量, 因此也可称之为堵水刚度. 本文采用围岩的原始渗水量来衡量围岩的抗渗性, 可将抗渗性定义为

$$K = \frac{P}{Q} \quad (1)$$

式中, P 为围岩受到的水头压力, Q 为原始渗水量.

在一定水头压力作用下, 围岩原始渗水量越大, 围岩抗渗性越弱, 反之围岩抗渗性越强. 在施工过程中, 海底隧道围岩渗流一般为高速非线性流动, 因此渗流规律无法用达西定律准确预测. 遗憾的是, 目前工程中采用的原始渗水量预测方法多基于达西定律推导. 本文首先构建隧道渗水量计算简化模型, 推导海底隧道原岩渗水量理论预测公式, 分析围岩抗渗性影响因素.

1.2 高速非线性流渗水量预测

1.2.1 基本假定及渗水量计算

在高水压裂隙岩体中, 地下水流态为惯性力占主导的高速非线性流^[22-23]. 为研究高速非线性流态下海底隧道涌水量, 做以下假定: (1) 隧道围岩为各向同性均匀介质; (2) 流体不可压缩, 且符合高速非线性流; (3) 地下水位水平且恒定; (4) 隧道断面为圆形. 海底隧道计算简图如图 1 所示, 采用等效面积法将非圆形隧道断面简化为圆形断面. 隧道等效开挖半径为 r , 海水深度为 h_w , 隧道中心距海床面 h , 围岩渗透系数为 k . 本文基于地下水动力学理论, 采用竖井法进行理论分析, 计算模型如图 2, H 为远场稳定水头, $H = h_w + h$.

本文采用幂函数型 Izbash 方程对高速非达西渗流场中隧道涌水量进行推导, 即在高水压裂隙岩体中水力梯度与渗流速度的关系^[24] 为

$$v = (ki)^{\frac{1}{m}} \quad (2)$$

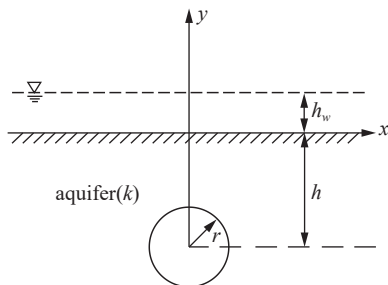


图 1 海底隧道简化模型

Fig. 1 Simplified model of subsea tunnels

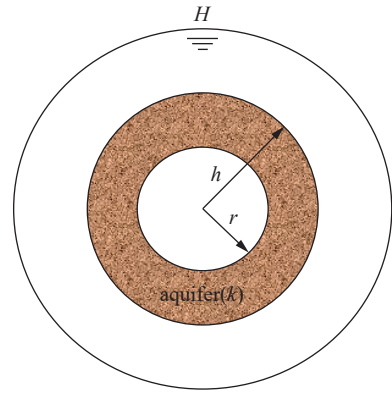


图 2 竖井法计算模型

Fig. 2 Calculation model of vertical shaft method

$$i = \frac{\partial \phi}{\partial \rho} \quad (3)$$

式中, k 为岩体渗透系数; m 为经验系数, 与流体流态有关, 当 $m = 1$ 时, 该式简化为适用于达西定律的线性渗流公式, 当 $1 < m \leq 2$ 时, 该式适用于由惯性力主导的非线性渗流.

根据渗流力学原理, 有平面径向渗流连续方程^[25]

$$\frac{\partial v}{\partial \rho} + \frac{v}{\rho} = 0 \quad (4)$$

式中, ρ 为围岩内任一点到隧道中心的距离, v 为围岩内任一点的渗流速度. 将式 (2) 和式 (3) 代入式 (4), 可得满足高速非线性渗流的连续方程

$$\frac{\partial \left(k \frac{\partial \phi}{\partial \rho} \right)^{\frac{1}{m}}}{\partial \rho} + \frac{1}{\rho} \left(k \frac{\partial \phi}{\partial \rho} \right)^{\frac{1}{m}} = 0 \quad (5)$$

式 (4) 的通解为

$$\phi = \frac{C_1}{1-m} \rho^{1-m} + C_2 \quad (6)$$

其中, C_1 和 C_2 为常数, 可由以下边界条件求出

$$\left. \begin{array}{l} \phi|_{\rho=r} = 0 \\ \phi|_{\rho=h} = h_w \end{array} \right\} \quad (7)$$

由式 (6) 和式 (7) 可得常数 C_1 和 C_2

$$\left. \begin{array}{l} C_1 = \frac{1-m}{h^{1-m} - r^{1-m}} h_w \\ C_2 = \frac{r^{1-m}}{r^{1-m} - h^{1-m}} \end{array} \right\} \quad (8)$$

则水头高度 ϕ 可表示为

$$\phi = \frac{h_w}{h^{1-m} - r^{1-m}} \rho^{1-m} + \frac{r^{1-m}}{r^{1-m} - h^{1-m}} \quad (9)$$

根据渗流力学原理, 无限平面内单孔圆形隧道渗流可表示为

$$Q = 2\pi r v \quad (10)$$

将式(2)和式(3)代入式(10)得满足高速非线性渗流的微分方程

$$Q = 2\pi r \cdot \left(k \frac{\partial \phi}{\partial \rho} \right)^{\frac{1}{m}} \quad (11)$$

将式(9)代入式(11), 即可得到基于 Izbash 方程的高速非线性渗流涌水量表达式

$$Q = 2\pi \cdot \left[\frac{(1-m) h_w k}{h^{1-m} - r^{1-m}} \right]^{\frac{1}{m}} \quad (m > 0 \text{ and } m \neq 1) \quad (12)$$

1.2.2 退化分析及数值模拟验证

假设渗流满足达西定律, 利用洛必达法则可得

$$Q = 2\pi \cdot \left[\frac{(1-m) h_w k}{h^{1-m} - r^{1-m}} \right]^{\frac{1}{m}} \Big|_{m \rightarrow 1} = \frac{2\pi h_w k}{\ln h - \ln r} \quad (13)$$

式(13)与文献[2]计算结果相同, 表明式(12)可退化为满足达西定律的隧道涌水量计算公式, 初步验证了本文涌水量计算公式的合理性。

为验证解析模型的准确性, 将所得到的解析解与数值解进行了比较。采用有限差分软件 FLAC^{3D}进行数值计算。假设一海底隧道等效半径为 $r = 5.5 \text{ m}$, 隧道拱顶距基岩距离为 20 m , 即 $h = 25.5 \text{ m}$, 海水深度 $h_w = 30 \text{ m}$, 考虑计算时间与精度, 模型尺寸取 $300 \text{ m} \times 150 \text{ m} \times 1 \text{ m}$ (长 \times 高 \times 宽), 模型边界条件为: 模型上边界即海床表面, 孔隙水压力为 0.3 MPa , 隧道内壁水压力为 0 MPa , 左右边界为透水边界。

在原岩渗透系数改变时, 将相关参数代入式(12)和式(13)求解, 对比数值解、退化线性解析解和非线性渗流解析解, 如图3所示。结果发现, 本文数值解和退化线性解析解的结果基本吻合, 隧道渗水量随着原岩渗透系数的升高而增大, 验证了本文非线性渗流解析解的正确性。数值解略高于退化线性解析解, 可能原因为数值模型隧道断面为六心圆隧道断面, 断面中心较正圆断面低, 因此渗水量较大。非线性渗流解析解结果明显大于数值解和退化线性解析解, 符合高速非线性渗流特征, 利用本文提出的非线性渗流解析解, 可计算高水压条件下海底隧道裂隙岩体渗水量。

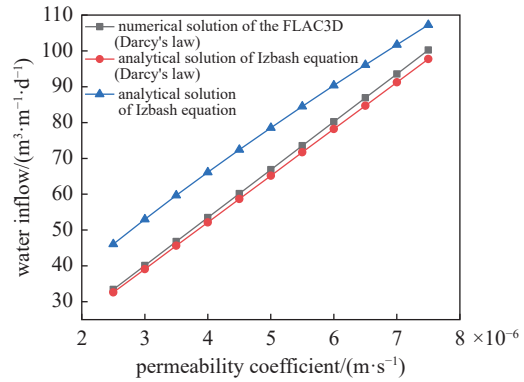


图3 数值解、退化线性解和非线性模型解关于渗透系数对海底隧道渗水量的影响

Fig. 3 Influences of permeability coefficient on water inflow of numerical solutions, degraded linear solutions, and nonlinear model solutions

1.3 围岩抗渗性影响因素的选取

由式(12)可知, 隧道原岩渗水量与岩体渗透系数、海水深度、岩石覆盖层高度和隧道半径有关, 且系数 m 与流体流态有关, 裂隙岩体中流体流态受裂隙粗糙度、几何特征等因素综合影响。由此可知, 围岩抗渗性分级与围岩分级存在根本差别。围岩分级是对围岩强度的评价, 主要由岩石坚硬程度和岩体完整性确定。而围岩抗渗性分级是对围岩渗水量的评价, 需由隧道所处的水文地质条件和岩体的渗透能力来确定。若围岩级别低, 但隧道所处水头高, 其抗渗性级别可能会高; 若围岩级别低, 完整性较好, 但其节理形成的过水通道条件好, 渗透能力强, 其抗渗性级别反而高。因此, 对围岩抗渗性分级非常重要且十分必要。

影响围岩抗渗性的因素较多, 虽然工程分类系统可以包含主要影响因素, 但是采用影响因素过多会使分类过程过于繁琐且无必要。同时, 还需考虑到这些因素在现场调查阶段收集的难易性以及在后续设计施工阶段的实用性。根据理论分析及现场调查总结, 需合理准确地选取能够代表岩体渗透能力、隧道所处的水文地质条件及隧道特征3方面的主要影响因素^[26-27]。

由于围岩渗透系数现场调查阶段收集较难, 需通过现场试验或室内试验确定。隧道围岩的渗透能力主要受岩石的性质和岩石裂隙发育程度影响, 可选用岩石饱和抗压强度和体积节理数表征。因此, 最终确定隧道围岩抗渗性的影响因素为岩石覆盖层厚度、水头高度、隧道半径、岩石单轴饱和抗压强度以及体积节理数。

1.4 现场检测统计数据

本文收集了 35 座水下及富水隧道 52 个典型断面的渗水案例, 统计了隧道渗水量、岩石覆盖层厚度、水头高度、隧道半径、岩石单轴饱和抗压强度以及围岩体积节理数, 具体数据如表 1 所示。

所统计的隧道围岩抗渗性随围岩所处的水文地质条件参数、围岩渗透能力参数和隧道特征参数的变化规律如图 4 所示。

由图 4 分析可知: (1) 在较小覆盖层厚度范围内, 隧道极易发生突涌水, 隧道围岩渗水量随覆盖层厚

表 1 现场监测统计数据

Table 1 Statistics of tunnel field monitoring

| No. | Tunnel name | Water inflow/ (m ³ ·d ⁻¹ ·m ⁻¹) | Overburden sickness/m | Hydraulic head/m | Tunnel radius/m | Equivalent permeability coefficient/(10 ⁻⁷ m·s ⁻¹) | R _c / MPa | Joint count/ (10 ⁵ Pa·m ⁻¹) |
|-----|--|--|--------------------------|---------------------|--------------------|--|-------------------------|---|
| 1 | Qingdao-Jiaozhou Bay Subsea Tunnel YK6 + 905 | 4.11 | 26.20 | 68.90 | 5.55 | 23.50 | 43.50 | 21 |
| 2 | Qingdao-Jiaozhou Bay Subsea Tunnel fault zone | 18.58 | 32.00 | 67.00 | 5.55 | 8.50 | 39.90 | 15 |
| 3 | Qingdao-Jiaozhou Bay Second Subsea Tunnel SK8 + 220 | 2.92 | 55.00 | 65.00 | 6.38 | 2.89 | 105.00 | 8 |
| 4 | Qingdao-Jiaozhou Bay Second Subsea Tunnel SK10 + 060 | 58.42 | 125.00 | 170.00 | 6.38 | 57.9 | 39.00 | 45 |
| 5 | Qingdao Metro Line 1 Tunnel | 3.34 | 41.85 | 84.27 | 5.17 | 10.3 | 45.20 | 20 |
| 6 | Qingdao Metro Line 3 Tunnel | 2.40 | 16.00 | 15.10 | 3.50 | 5.79 | 40.00 | 10 |
| 7 | Qingdao Metro Line 8 Tunnel | 11.26 | 45.00 | 51.00 | 4.72 | 34.7 | 35.20 | 29 |
| 8 | Xiamen Xiang'an Subsea Tunnel weathered slot F1 | 11.01 | 36.90 | 54.90 | 6.36 | 21.4 | 80.00 | 25 |
| 9 | Xiamen Xiang'an Subsea Tunnel weathered slot F4 | 82.80 | 18.64 | 63.64 | 6.36 | 500 | 25.00 | 50 |
| 10 | Xiamen Haicang Tunnel weathered slot | 2.70 | 39.06 | 43.06 | 7.46 | 100 | 125.00 | 35 |
| 11 | Xiamen Haicang Tunnel K9 + 260 | 8.29 | 27.66 | 54.53 | 7.46 | 7.06 | 118.00 | 14 |
| 12 | Xiamen Haicang Tunnel K9 + 800 | 7.63 | 25.66 | 49.46 | 7.46 | 7.06 | 108.00 | 13 |
| 13 | Xiamen Metro Line 3 undersea section | 1.82 | 27.20 | 46.00 | 3.35 | 347 | 60.00 | 34 |
| 14 | Shantou Bay Tunnel | 8.04 | 12.40 | 22.40 | 7.50 | 5.79 | 125.00 | 10 |
| 15 | Zhanjiang Bay Subsea Tunnel | 14.59 | 17.60 | 53.10 | 6.90 | 0.03 | 11.00 | — |
| 16 | Eastern Shenzhen Bypass Expressway | 11.38 | 40.40 | 29.80 | 6.00 | 15.60 | 29.00 | 21 |
| 17 | Pearl River Estuary Railway Tunnel | 9.60 | 115.00 | 115.00 | 5.09 | 5.79 | 107.50 | 10 |
| 18 | Lion Rock Subsea Tunnel | 7.39 | 26.00 | 52.60 | 5.40 | 6400 | 82.80 | 3 |
| 19 | Changsha Metro Line 3 | 8.65 | 19.50 | 17.40 | 3.00 | 23.10 | 46.00 | 24 |
| 20 | Qiyueshan Expressway Tunnel | 84.72 | 273.14 | 227.00 | 4.98 | 4.00 | 28.00 | 55 |
| 21 | Xuefeng Mountain Tunnel (left line) | 1.74 | 495.00 | 455.00 | 3.69 | 0.683 | 129.60 | 3 |
| 22 | Xuefeng Mountain Tunnel (right line) | 2.46 | 412.00 | 375.00 | 3.69 | 0.521 | 127.00 | 3 |
| 23 | Huaying Mountain Tunnel | 74.22 | 220.00 | 180.00 | 5.00 | 20.00 | 41.70 | 48 |
| 24 | Yuanliangshan Tunnel | 28.77 | 560.00 | 460.00 | 6.00 | 5.00 | 51.00 | 42 |
| 25 | Gele Mountain Tunnel | 13.09 | 25.00 | 23.00 | 2.82 | 15.00 | 75.50 | 20 |
| 26 | Shenhe Plateau Tunnel | 1.13 | 81.40 | 60.60 | 2.55 | 3.00 | 10.00 | — |
| 27 | Shaoling Plateau Tunnel | 1.73 | 130.00 | 70.00 | 2.55 | 4.00 | 9.00 | — |
| 28 | Bailu Plateau Tunnel | 0.53 | 282.22 | 222.02 | 2.55 | 0.40 | 12.00 | — |
| 29 | Nankun Railway Tunnel | 15.20 | 69.50 | 62.50 | 3.52 | 20.60 | 70.00 | 30 |
| 30 | Zhongliang Mountain Tunnel (Chongqing-Suihua Expressway) | 7.99 | 290.00 | 150.00 | 4.49 | 67.70 | 100.80 | 36 |

续表1

| No. | Tunnel name | Water inflow/ (m ³ ·d ⁻¹ ·m ⁻¹) | Overburden sickness/m | Hydraulic head/m | Tunnel radius/m | Equivalent permeability coefficient/(10 ⁻⁷ m·s ⁻¹) | R _c / MPa | Joint count/ (10 ⁵ Pa·m ⁻¹) |
|-----|--|--|--------------------------|---------------------|--------------------|--|-------------------------|---|
| 31 | Zhongjiang Mountain Tunnel (Chongqing-Xiangyang Expressway) | 6.25 | 220.00 | 190.00 | 2.50 | 1.77 | 116.00 | 8 |
| 32 | Maluqing Tunnel | 2.00 | 270.00 | 122.45 | 5.51 | 22300 | 95.50 | 40 |
| 33 | Cangling Tunnel (Xianju section) | 77.76 | 412.00 | 372.00 | 5.03 | 3090 | 32.50 | 52 |
| 34 | Cangling Tunnel (Jinyun Hengxi section) | 44.14 | 663.00 | 357.14 | 5.03 | 1070 | 60.00 | 45 |
| 35 | Bieyan Trench Tunnel DK403 + 982 | 16.65 | 112.00 | 91.84 | 5.43 | 0.70 | 21.00 | 3 |
| 36 | Bieyan Trench Tunnel DK404 + 225 | 9.60 | 163.00 | 102.04 | 5.43 | 0.06 | 78.50 | 1 |
| 37 | Bieyan Trench Tunnel DK404 + 423 | 40.00 | 202.00 | 91.84 | 5.43 | 1.00 | 62.00 | 43 |
| 38 | Bieyan Trench Tunnel DK404 + 473 | 19.52 | 211.00 | 66.33 | 5.43 | 0.02 | 70.00 | 38 |
| 39 | Mingyue Mountain Tunnel K5 + 573 | 3.60 | 150.00 | 125.92 | 5.50 | 0.160 | 73.00 | 2 |
| 40 | Wankai Zhoujiaba-Puli Express Tunnel ZK4 + 393 | 65.20 | 542.00 | 163.27 | 3.56 | 926 | 45.00 | 46 |
| 41 | Tiefengshan No. 2 Tunnel | 5.81 | 553.00 | 406.00 | 3.56 | 0.320 | 120.00 | 2 |
| 42 | Dabie Mountain Tunnel YK19 + 670 | 32.73 | 358.00 | 221.00 | 4.60 | 8500 | 100.00 | 35 |
| 43 | Dabie Mountain Tunnel YK20 + 015 | 37.50 | 443.00 | 307.00 | 4.60 | 156 | 42.00 | 40 |
| 44 | Dabie Mountain Tunnel YK20 + 050 | 60.00 | 482.00 | 398.00 | 4.60 | 300 | 40.00 | 44 |
| 45 | Daxiangling Tunnel F3 fault zone | 1.81 | 250.00 | 92.50 | 5.16 | 2.31 | 133.00 | 5 |
| 46 | Daxiangling Tunnel FX2 fault zone | 2.65 | 280.00 | 142.86 | 5.16 | 4.63 | 130.00 | 9 |
| 47 | Daxiangling Tunnel FX3 fault zone | 3.30 | 152.00 | 61.22 | 5.16 | 8.10 | 128.00 | 11 |
| 48 | Tianjin Metro Line 6 Youyi Road | 23.41 | 18.80 | 14.20 | 3.10 | 113 | 46.00 | — |
| 49 | Tianjin Metro Line 6 Guo Huangzhuang South | 4.75 | 18.00 | 8.70 | 3.10 | 15.00 | 24.00 | — |
| 50 | Tianjin Metro Line 6 Terminal Station | 7.34 | 16.70 | 12.00 | 3.10 | 22.00 | 21.00 | — |
| 51 | Dujia Mountain Tunnel | 1.20 | 80.00 | 60.00 | 3.00 | 3.50 | 40.00 | 6 |
| 52 | Chikushi Tunnel | 3.77 | 300.00 | 253.00 | 0.50 | 5.00 × 10 ⁻⁸ | 131.00 | 3 |

度增加而下降, 主要原因一是由达西定律可知覆盖层导致水头损失增大, 二是覆盖层厚度过小极大地限制了注浆压力, 影响到隧道围岩注浆效果; 在覆盖层厚度较大时, 需考虑到覆盖层厚度直接影响围岩水压, 水载荷相应增加, 围岩渗水量增加。同时覆盖层越厚, 出现隔水层的概率也越大, 这对隧道堵水更有利。

(2) 随着水头高度的增加, 隧道围岩渗水量上升。这是由于水头高度直接影响围岩承受的水压力的大小, 上覆水层越高, 作用于围岩的水压力越大。隧道围岩承受的静水压力增大使得岩土体的有效应力减小, 岩土体更易发生变形和破坏, 隧道发生渗流和涌水的可能性增大。

(3) 隧道围岩涌水量与隧道半径相关性较弱, 其原因是隧道防排水设计按照行业规范要求, 在相同

的防水区段内渗水量控制标准一致且具有较强的经验性, 通过采取注浆堵水后渗水量得到有效控制。

(4) 隧道围岩渗水量随围岩体积节理数的增大而上升。岩体渗流本质是流体在不连续面和其组成网络中的流动, 而节理裂隙作为一类典型的岩体不连续面, 其发育程度对围岩渗水量影响很大。围岩体积节理数越大, 其可能形成的渗水通道越多, 透水能力越强, 其渗水量越大。

(5) 随着岩石单轴饱和抗压强度增加, 隧道围岩渗水量降低。岩石的单轴饱和抗压强度是岩体分级的重要指标, 代表了岩体的强度与稳定性, 常用其衡量岩石的坚硬程度。围岩在受压状态下产生细观微裂纹并逐渐累积形成宏观破裂^[28], 给岩土体间自由水提供了通道, 因此岩石的强度与堵水能力有密切关系。

对上述数据中隧道渗水量进行统计分析,如图5所示。图中统计数据呈正态分布表明数据具有一定的代表性,箱线图以上下四分位数和四分位距来判别异常值,异常值的出现可能是由于隧道所在位置水压过高且地质条件差导致突涌水事故的发生。由图可知统计数据渗水量多集中于0~20 m³/(d·m),上四分位值为22.28 m³/(d·m),下四分位值为3.32 m³/(d·m),中位数值为8.47 m³/(d·m),代表样本数据的平均水平。

鉴于箱线图具有一定的耐抗性^[29],根据箱线图给出的上四分位值、中位数和下四分位值对统计的

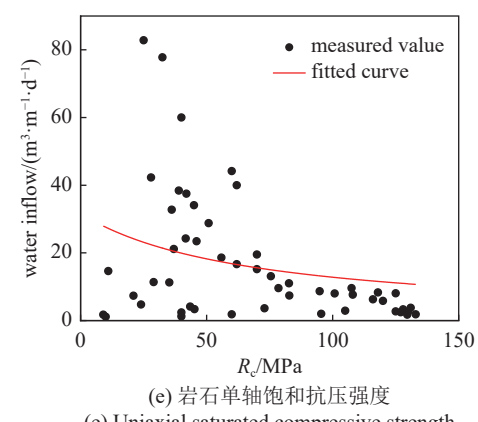
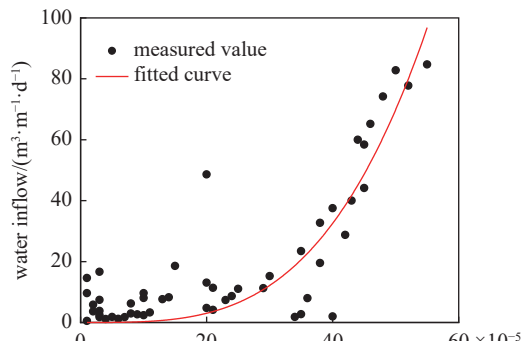
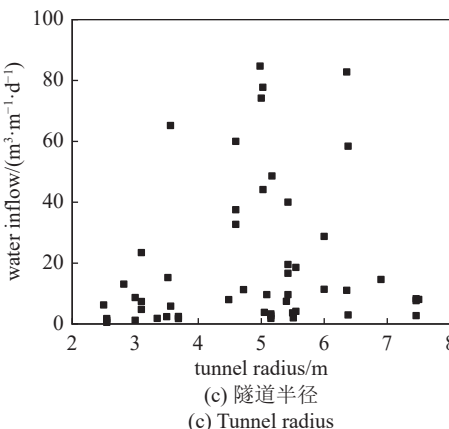
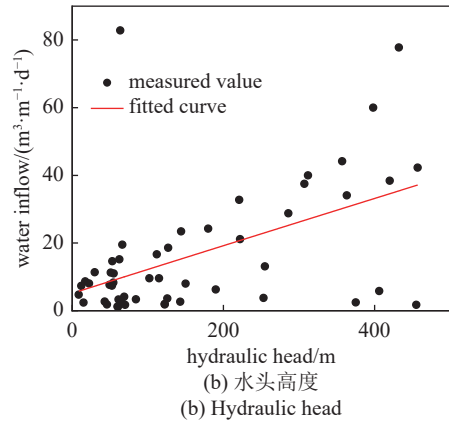
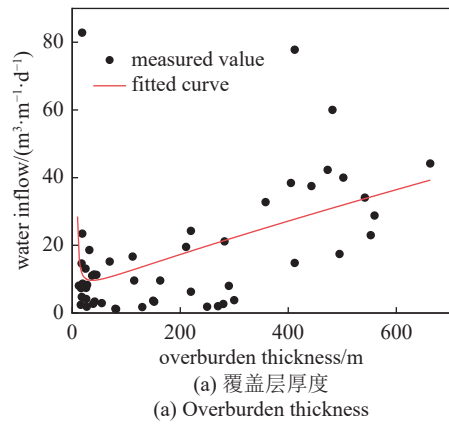


图4 围岩抗渗性影响因素

Fig. 4 The influencing factors of the anti-seepage of surrounding rock

隧道围岩渗水量进行划分,分别用I, II, III和IV表示,如表2所示。对于隧道涌水量的分级,国内外学者都提出了不同的分类标准,通过对比可知本文的划分标准有一定可行性。

根据上述确定的围岩渗水量影响因素及分级方法对样本数据进行分析可得相关系数图,如图6所示。由于数据间存在非线性关系,且一组数据为等级类型,相关性分析采用斯皮尔曼相关系数计算,计算公式如下

$$\rho = 1 - \frac{6 \sum d_i^2}{n(n^2 - 1)} \quad (14)$$

其中, d_i 为第 i 个数据对的秩次差, n 为样本数量。

由图6可知,各影响因素与涌水量级别的相关系数均较低,其中覆盖层厚度、水头高度和体积节理数与级别正相关,岩石单轴饱和抗压强度与级别负相关,这也与上一节对样本数据进行拟合分析后得到的规律相印证。影响因素中水头高度与覆盖层厚度相关系数较大是由于海底隧道岩石覆盖层厚度

表 2 隧道围岩涌水量分级方法

Table 2 Classification method for tunnel surrounding rock water inflow

| this paper | SGR ^[30] | code for design of railway tunnel ^[31] | RSR ^[32] | RMR ^[32] | fuzzy Delphi AHP method ^[33] | Level |
|--------------|---------------------|---|---------------------|---------------------|---|--|
| | | | | | | Water inflow/(m ³ ·d ⁻¹ ·m ⁻¹) |
| 0 ~ 3.32 | 0 ~ 3.46 | 0 ~ 1.44 | 0 ~ 4.32 | 0 ~ 1.44 | 0 ~ 1.73 | I (humidity) |
| 3.32 ~ 8.47 | 3.46 ~ 8.64 | 1.44 ~ 3.6 | 4.32 ~ 21.6 | 1.44 ~ 3.6 | 1.73 ~ 8.64 | II (dripping water) |
| 8.47 ~ 22.28 | 8.64 ~ 13.82 | 3.6 ~ 18 | > 21.6 | 3.6 ~ 18 | 8.64 ~ 15.55 | III (linear flow) |
| > 22.28 | 13.82 ~ 24.19 | > 18 | — | > 18 | 15.55 ~ 25.92 | IV (gushing water) |
| — | > 24.19 | — | — | — | > 25.92 | V |

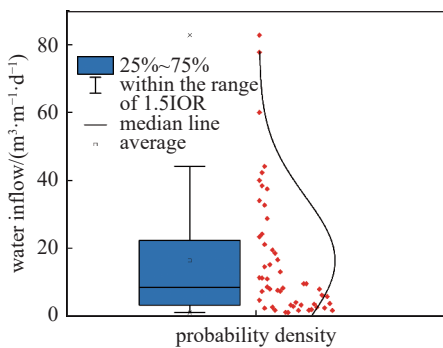


图 5 隧道渗水量箱线图

Fig. 5 The box plot of tunnel seepage quantity

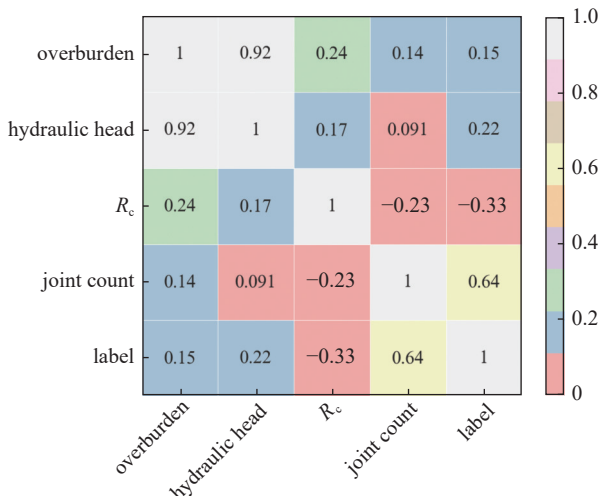


图 6 各影响因素及类别间相关系数图

Fig. 6 Correction coefficient diagram among influencing factors and level

增加会直接导致水头高度增大。

2 基于决策树的围岩抗渗性分级方法

针对海底隧道围岩涌水量影响因素, 建立前述 4 个评价指标与抗渗性的关系, 提出抗渗性分级方法, 并提出相应的排水量控制标准和处置方案。相较

于其他监督学习统计方法, 决策树算法可对连续值属性实现多元分类回归, 能够很好地处理具有非线性关系的特征及其中的缺失数据, 且具有可读性, 可较好解决隧道围岩抗渗性分级问题。

2.1 C4.5 决策树分类算法基本原理

(1) 决策树模型

决策树分类模型是一种对已有样本数据进行分类的树形结构, 如图 7 所示。根结点包含所有样本数据, 从根结点开始对数据按照特定规则分流到内部结点, 每一个内部结点都对应一个分类的特征取值, 如此递归直至满足终止条件到达叶结点, 叶结点表示一个类^[34]。按照该方法构建的树状结构每次分流都能使数据更趋于同类, 且树状结构的每一条路径都是互斥且互补的, 亦即决策树能使每个数据的分流有且只有一条路径。

(2) C4.5 算法连续属性特征选择

特征选择的要点在于选取对训练数据具有分类能力的最优特征, 以此提高决策树的分类效率。对于每一次内部结点内数据分类, 都希望下一个结点所包含的数据尽可能属于同一类别, 即“纯度”更高。信

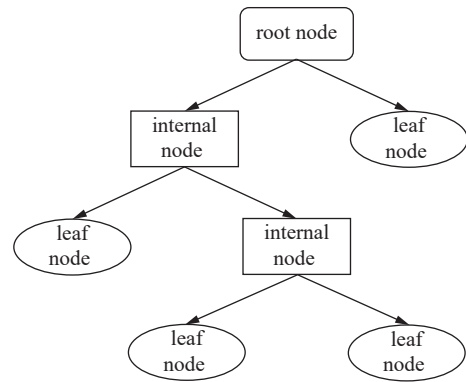


图 7 决策树结构图

Fig. 7 Decision tree structure diagram

息熵可以度量随机变量不确定性, 是度量样本集合纯度最常用的指标之一, 其值越小, 样本集合纯度越高^[35]. 设样本集合 D 中第 k 类样本所占的比例为 p_k ($k = 1, 2, \dots, n$), 则定义集合 D 的信息熵为

$$Ent(D) = - \sum_{k=1}^n p_k \log_2 p_k \quad (15)$$

对于连续属性, 可取值数目无限多, 不能直接根据连续属性的可取值对结点内样本数据进行划分, 因此考虑采用二分法对连续属性进行离散化^[36-37]. 设样本集合 D 中连续属性 a 有 n 个不同取值, 对 n 个值从小到大进行排序, 记为 $\{a^1, a^2, \dots, a^n\}$. 定义 $n-1$ 个划分点 t 所在集合为

$$T_a = \left\{ \frac{a^i + a^{i+1}}{2} \mid 1 \leq i \leq n-1 \right\} \quad (16)$$

划分点 t 将 D 划分为 D_t^+ 和 D_t^- , 其中 D_t^+ 包含连续属性 a 上取值大于 t 的样本, D_t^- 包含连续属性 a 上取值小于等于 t 的样本.

此时便可将 t 看做离散属性值, 根据式 (15) 计算出 D_t^+ 和 D_t^- 的信息熵, 考虑到两个分支结点包含样本数量不同, 赋予分支结点权重 $|D_t^+|/|D|$, 即样本数量越多分支结点影响越大, 由此可计算出每个划分点 t 的信息增益, 选取连续属性 a 中信息增益最大即纯度最高的划分点 t 为最优划分点, 即

$$Gain(D, a) = \max_{t \in T_a} \left[Ent(D) - \sum_{\lambda \in \{-, +\}} \frac{|D_t^\lambda|}{|D|} Ent(D_t^\lambda) \right] \quad (17)$$

(3) 决策树的生成

对已知训练数据集 $D = \{(x_1, y_1), (x_2, y_2), \dots, (x_n, y_n)\}$, x_i ($i = 1, 2, \dots, n$) 为 m 维向量, 属性集 $A = \{a_1, a_2, \dots, a_m\}$.

①若 D 中样本全属于同一类别, 则将结点标记为该类别叶节点.

②若不属于①所述情况, 根据式 (15) ~ 式 (17) 得到的信息增益, 从所有划分点中找出信息增益最高为最优划分点. 根据该划分点将 D 进行分类生成子集 D_v , 成为新的结点.

③若某个子集 D_v 中所有数据均属于同一类别, 则无需进行分类, 直接标记为该类别叶节点.

④若子集 D_v 中数据仍有大量数据属于不同类别, 则重复②和③操作递归生成决策树的分支, 直至产生的结点均为叶节点.

⑤输出决策树.

2.2 隧道围岩抗渗性分级方法

根据第 1 节分析可确定岩石覆盖层厚度、水头高度、体积节理数和岩石单轴饱和抗压强度为围岩抗渗性的 4 个评价指标属性, 表示为 $A = \{a_1, a_2, a_3, a_4\}$, 且均为连续属性. 同时将围岩根据渗水量分为 4 个等级, 即 $y_i \in \{\text{I}, \text{II}, \text{III}, \text{IV}\}$ ($i = 1, 2, \dots, n$).

(1) 属性划分选择

采用 2.1 节 (3)②中方法对数据集进行比较划分. 以根结点岩石覆盖层厚度属性为例, 首先采用式 (16) 对覆盖层厚度取值进行离散化处理, 再采用式 (15) 和式 (17) 计算该属性各候补划分点信息增益, 岩石覆盖层厚度部分信息增益 (按信息增益降序) 见表 3. 由此可得根结点样本数据划分点为覆盖层厚度大于 220 m.

表 3 部分岩石覆盖层厚度划分点信息增益

Table 3 Information gain of overburden division points

| Splitting point | Information gain |
|-----------------|------------------|
| 220.00 | 0.302895712 |
| 215.50 | 0.236562694 |
| 412.00 | 0.215919612 |
| 235.00 | 0.211351419 |
| 260.00 | 0.202191118 |
| 329.00 | 0.200234818 |
| | |
| 18.722 | 0.027855219 |
| 25.3315 | 0.027847104 |
| 19.15 | 0.024835007 |

(2) 生成决策树

将原始样本数据集以 4:1 的比例拆分为训练集和测试集, 训练集数据按照上述方法递归生成决策树如图 8, 测试集数据对生成的决策树进行模型评估, 得到准确率为 90.91%, 表明模型预测效果较好.

2.3 围岩处置方案建议

海底隧道水源充足, 围岩持续承受高水压作用, 且多采用“V”型纵坡, 无法自然排水, 因此对海底隧道防排水设计提出“堵水限排”的设计理念, 以减少地下水的排放量, 并降低隧道衬砌所承受的水压力.

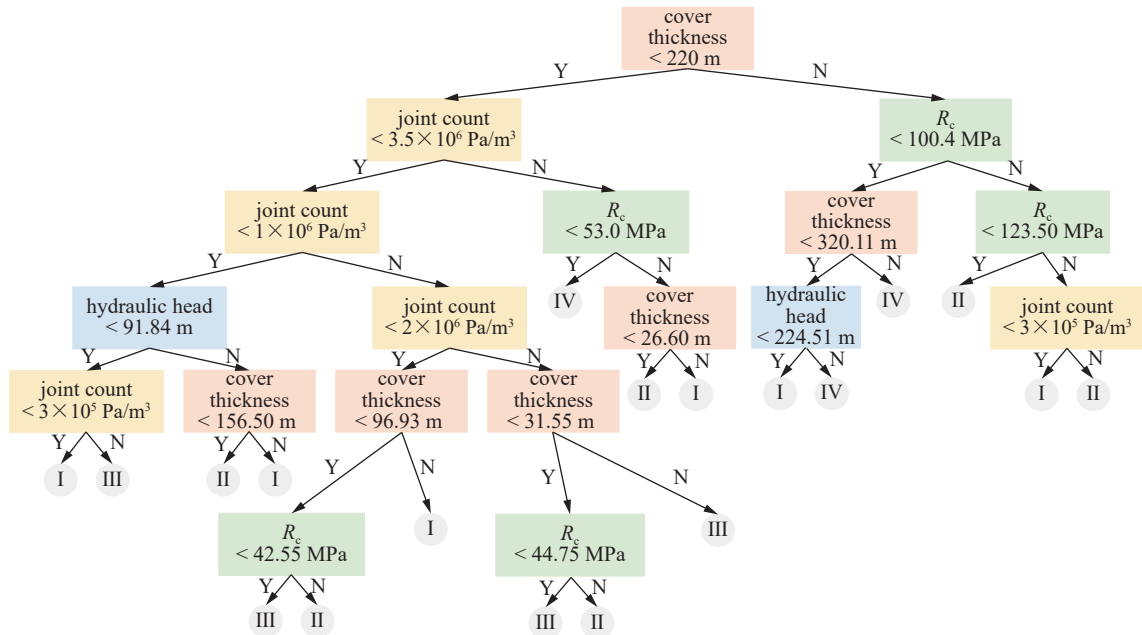


图 8 抗渗性分级决策树

Fig. 8 Anti-seepage classification decision tree

对于不同抗渗性等级的围岩, 考虑到注浆加固圈堵水率一般为 90%^[2], 并参考相关工程经验, 给出了隧

道渗水量控制标准, 本文提出相应的工程建议如表 4 所示。

表 4 不同抗渗性级别围岩加固与支护方案建议

Table 4 Proposed support scheme of different anti-seepage conditions of surrounding rock

| Surrounding rock anti-seepage classification | Characteristics of the surrounding rock and water discharge conditions | Reinforcement methods and requirements | Allowable discharge control standards/ ($m^3 \cdot d^{-1} \cdot m^{-1}$) | Tunnel support design recommendations |
|--|--|--|--|---|
| I | Surrounding rock has high strength with poorly developed structural surfaces, well or moderately bonded, and rock mass exhibits a massive or very thickly bedded structure. Alternatively, surrounding rock may have extremely high strength, with poorly bonded structural surfaces, and rock mass exhibits a blocky or thickly bedded structure. The surrounding rock may be dry or damp, with only minor localized seepage observed at the face after excavation. The water pressure is less than 0.1 MPa. Surrounding rock exhibits moderate strength, with relatively developed structural surfaces, well or moderately bonded, rock mass exhibits a blocky structure. Alternatively, surrounding rock may have high strength and poorly bonded structural surfaces, rock mass exhibits a fractured blocky or medium-thick bedded structure. There is localized drip seepage from the surrounding rock, with occasional outflow of infill from joints, and the water pressure ranges from 0.1 to 0.25 MPa. | Construction in accordance with design specifications. | 0 ~ 0.1 | Conduct construction in accordance with design specifications |
| II | Surrounding rock has relatively low strength, with well-developed structural surfaces which is well or moderately bonded, rock mass exhibits a fragmented or thinly bedded structure. Alternatively, surrounding rock has a certain degree of strength, poorly bonded structural surfaces, and presents a fractured blocky structure. There is rainfall-like or linear flow seepage from the surrounding rock, with infill from joints occasionally flowing out, and the water pressure ranges from 0.25 to 1 MPa. | Construction in accordance with design specifications | 0.1 ~ 0.3 | When there is localized seepage on the surface of the initial support, localized radial grouting should be employed |
| III | | Full-face grouting should be applied 30 meters ahead, with a 3 to 5 meters reinforcement range. If the face is locally fragmented, advanced peripheral grouting may be considered, with a grouting length of 30 meters and a reinforcement range of 3 to 5 meters. Alternatively, advance local grouting can be adopted, supplemented by radial grouting if necessary. | 0.3 ~ 0.8 | Primary support should use shotcrete. Backfill grouting should be promptly conducted behind the initial support. The secondary lining can utilize high-performance waterproof concrete. |

续表4

| Surrounding rock anti-seepage classification | Characteristics of the surrounding rock and water discharge conditions | Reinforcement methods and requirements | Allowable discharge control standards/ ($\text{m}^3 \cdot \text{d}^{-1} \cdot \text{m}^{-1}$) | Tunnel support design recommendations |
|--|---|--|---|--|
| IV | Surrounding rock has low strength, with highly developed structural surfaces, generally or poorly bonded. The rock mass exhibits a fragmented or loose structure. During the surrounding rock blasting, a gushing water flow or pressurized water may occur, with water pressure exceeding 1 MPa. | Full-face grouting should be performed 30 meters ahead, with a reinforcement range extending 6 to 8 meters. After excavation, radial grouting with range of 2 to 3 meters should be applied. | 0.8 ~ 2.5 | Primary support should employ shotcrete of the impermeability grade higher than P12. Backfilling and grouting should promptly be conducted behind the initial support. Advanced grouting techniques and materials should be used, and the secondary lining can use high performance waterproof concrete. |

3 工程应用

青岛胶州湾第二海底隧道横跨胶州湾连接黄岛端与青岛端, 是青岛市中心城区“六横九纵”高快速路网的重要组成部分, 其地质剖面图如图9所示。隧道海域段里程为SK7 + 578 ~ SK17 + 995, 采用钻爆法和盾构法组合施工, 其中海域钻爆段海水深8.5~45 m, 隧道覆盖层厚度55~125 m, 穿越地层以中微

风化花岗岩为主, 基岩上覆第四系覆盖层。隧道穿过沧口断裂带, 岩石多较破碎, 并形成透水通道, 易发生突涌水事故。

本文搜集了39个现场隧道断面的工程地质情况, 将各参数代入式(12)计算渗水量, 并与实测值进行对比, 如图10所示。结果显示, 本文解析解与实测值较吻合, 进一步验证了解析解的正确性。

采用本文提出的抗渗性分级方法对胶州湾第二

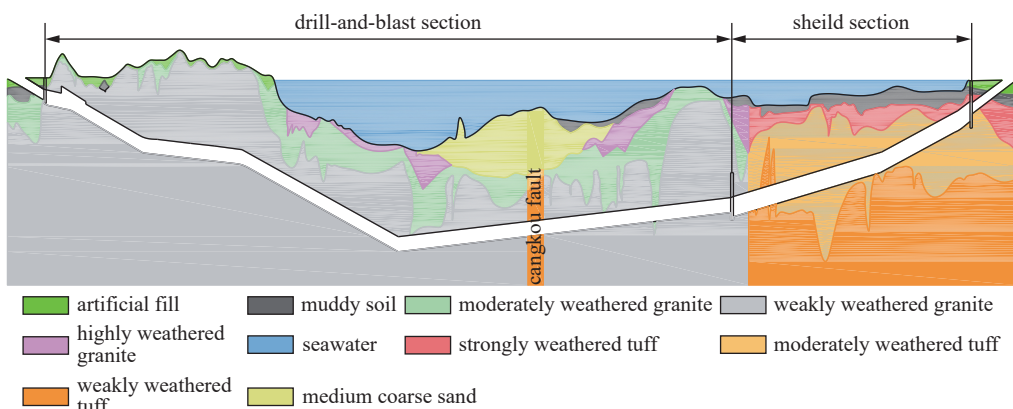


图9 胶州湾二隧地质剖面图

Fig. 9 Geological profile of the Qingdao-Jiaozhou Bay Second Subsea Tunnel

海底隧道钻爆法海域段(SK8 + 100 ~ SK14 + 740)

标高-120~-50 m岩体进行分级, 结果如图11所示(岩体抗渗性在空间上应为连续分布, 图中所示为部分区域预测结果)。由下图可知隧道岩体大部分抗渗性为II和III级, 极少数为I和IV级。SK11 + 860附近预测IV级区域为沧口断裂带, 构造破碎带不均匀发育, 具有岩性分布和接触关系复杂的特征, SK13 + 560附近预测IV级区域岩体为中风化花岗岩, 岩石岩性较差, 岩体呈砂砾状和角砾状, 图12为两个预测IV级区域钻孔岩心照片。以上预测抗渗性较差岩体与工程实际情况基本相符, 表明该分级方法具有一

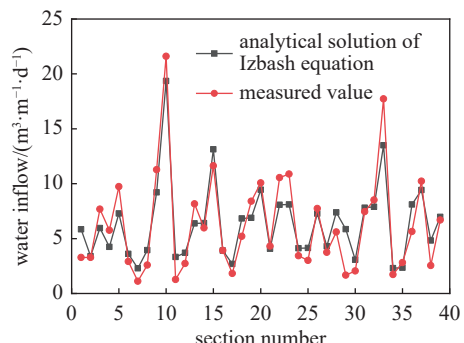


图10 工程实测值与非线性渗流解析解对比

Fig. 10 Comparison between engineering measured values and nonlinear seepage analytical solutions

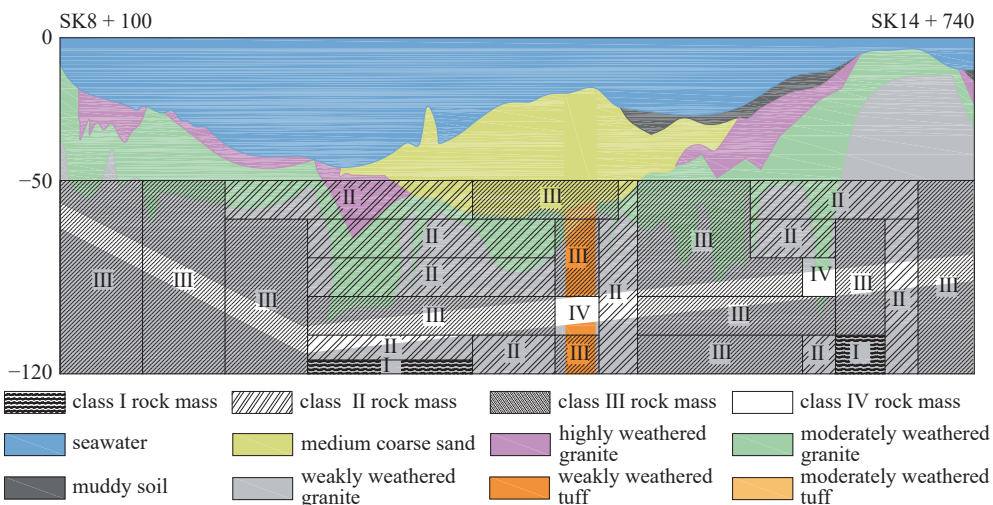


图 11 胶州湾第二海底隧道海域钻爆段岩体抗渗性分级

Fig. 11 The anti-seepage classification of surrounding rock in the drilling and blasting section of the Qingdao-Jiaozhou Bay Second Subsea Tunnel



图 12 钻孔揭示结果

Fig. 12 Borehole revealed results

定的参考价值。

4 结论

海底隧道围岩抗渗性的建立使得排水量控制标准的确定和可靠的分区防水成为可能,由此形成的抗渗性分级方法实现了防排水设计理论的新突破,为实现排水量的主动控制提供了理论支撑。

(1) 提出了围岩抗渗性的概念,定义为隧道围岩抵抗水流渗透的能力,并推导了施工期高速流动条件下裂隙岩体海底隧道原始渗水量预测公式,并分

析了岩体渗透能力、隧道所处的水文地质条件及隧道特征等对于围岩抗渗性的影响机制。

(2) 通过对 52 个典型水下隧道及富水隧道断面的渗水案例数据进行统计分析,确定了岩石覆盖层厚度、水头高度、岩石单轴饱和抗压强度以及体积节理数作为抗渗性分级指标,并采用四分法对隧道涌水量进行分级,作为围岩抗渗性分级参考。

(3) 通过对统计数据进行机器学习建立决策树预测模型,实现了连续属性数据的分级预测。将决策树预测模型应用于工程实际,结果表明决策树模型预测的围岩抗渗性级别与实际情况相近,采用该方法对围岩抗渗性分级简单直观,能够客观反映岩体抗渗性。

(4) 本文仅讨论了岩石覆盖层厚度、水头高度、岩石单轴饱和抗压强度以及体积节理数 4 种影响因素,实际上围岩裂隙发育情况对围岩抗渗性也至关重要,但鉴于围岩裂隙状况分类标准不够明确,且实际工程中勘察阶段收集数据较复杂,因此未予采用。在今后的工作中可结合机器学习对岩体裂隙图像进行智能识别,以便能够更加精确地对围岩抗渗性进行分级预测。

参 考 文 献

- 王梦恕, 皇甫明. 海底隧道修建中的关键问题. 建筑科学与工程学报, 2005, 4: 1-4 (Wang Mengshu, Huangfu Ming. Key problems on subsea tunnel construction. *Journal of Architecture and Civil Engineering*, 2005, 4: 1-4 (in Chinese))
- 张顶立, 孙振宇. 海底隧道主动控制式防排水系统及其设计方法.

- 岩石力学与工程学报, 2019, 38(1): 1-17 (Zhang Dingli, Sun Zhenyu. An active control waterproof and drainage system of subsea tunnels and its design method. *Chinese Journal of Rock Mechanics and Engineering*, 2019, 38(1): 1-17 (in Chinese))
- 3 《中国公路学报》编辑部. 中国交通隧道工程学术研究综述·2022. 中国公路学报, 2022, 35(4): 1-40 (Edition Department of China Journal of Highway and Transport. Review on China's traffic engineering research: 2022. *China J. Highw. Transp.*, 2022, 35(4): 1-40 (in Chinese))
- 4 张素磊, 鲍彤, Yoo Chungsik 等. 隧道复合式防排水系统的设计、试验及工程应用. 中国公路学报, 2021, 34(4): 198-208 (Zhang Sulei, Bao Tong, Yoo Chungsik, et al. Design, test, and engineering application of a composite waterproof and drainage system in tunnels. *China J. Highw. Transp.*, 2021, 34(4): 198-208 (in Chinese))
- 5 Li PF, Liu HC, Zhao Y, et al. A bottom-to-up drainage and water pressure reduction system for railway tunnels. *Tunnelling and Underground Space Technology*, 2018, 81: 296-305
- 6 Zhang Y, Zhang DL, Fang Q, et al. Analytical solutions of non-Darcy seepage of grouted subsea tunnels. *Tunnelling and Underground Space Technology*, 2020, 96: 103182
- 7 张明聚, 王思卿, 李鹏飞等. 考虑防排水系统的隧道渗流场解析. 隧道建设, 2023, 43(S1): 46-53 (Zhang Mingju, Wang Siqing, Li Pengfei, et al. Analysis of tunnel seepage field considering drainage system. *Tunnel Construction*, 2023, 43(S1): 46-53 (in Chinese))
- 8 Sun ZY, Zhang DL, Li MY, et al. Large deformation characteristics and the countermeasures of a deep-buried tunnel in layered shale under groundwater. *Tunnelling and Underground Space Technology*, 2024, 144: 105575
- 9 Li DK, Yu Y, Zheng JF, et al. Analytical study of steady state seepage in a circular tunnel considering the outer boundary of the grouting ring as a non-constant head boundary. *Tunnelling and Underground Space Technology*, 2024, 144: 105510
- 10 金波, 胡明, 方棋洪. 考虑渗流效应的深埋海底隧道围岩与衬砌结构应力场研究. *力学学报*, 2022, 54(5): 1322-1330 (Jin Bo, Hu Ming, Fang Qihong. Research on stress field of surrounding rock and lining structure of deep-buried subsea tunnel considering seepage effect. *Chinese Journal of Theoretical and Applied Mechanics*, 2022, 54(5): 1322-1330 (in Chinese))
- 11 Qin ZG, He WG, Zhou HG. Analytical study on seepage field of subsea twin tunnels constructed by NATM. *Ocean Engineering*, 2022, 264: 112345
- 12 柴宝红, 史红英, 梅坤等. 岩溶地区高速公路隧道绿色注浆试验研究. 交通科学与工程, 2022, 38(3): 107-112 (Chai Baohong, Shi Hongying, Mei Kun, et al. Study on green grouting test of highway tunnel in karst area. *Journal of Transport Science and Engineering*, 2022, 38(3): 107-112 (in Chinese))
- 13 刘翔, 纪敏龙, 王东池等. 双线非对称平行海底隧道非线性渗流场解析研究. 工程力学, 2024, DOI: 10.6052/j.issn.1000-4750.2024.02.0146 (Liu Xiang, Ji Minlong, Wang Dongchi, et al. Analytical solutions on non-darcy seepage of subsea twin-parallell asymmetric tunnels. *Engineering Mechanics*, 2024, DOI: 10.6052/j.issn.1000-4750.2024.02.0146 (in Chinese))
- 14 Liu X, Wang DC, Zhang Y, et al. Analytical solutions on non-Darcy seepage of grouted and lined subsea tunnels under dynamic water levels. *Ocean Engineering*, 2023, 267: 113276
- 15 Wang JC, Zhang DL, Sun ZY, et al. Control effect and optimization scheme of combined rockbolt-cable support for a tunnel in horizontally layered limestone: A case study. *Journal of Rock Mechanics and Geotechnical Engineering*, 2024, 16(11): 4586-4604
- 16 Kitamura A. Technical development for the Seikan tunnel. *Tunnelling and Underground Space Technology*, 1986, 1(3-4): 341-349
- 17 王建宇. 对隧道衬砌水压力载荷的讨论. 现代隧道技术, 2006, 43(S): 67-73 (Wang Jianyu. A discussion on water pressure loads acting on lining structures. *Modern Tunnelling Technology*, 2006, 43(S): 67-73 (in Chinese))
- 18 李鹏飞, 张顶立, 赵勇等. 海底隧道复合衬砌水压力分布规律及合理注浆加固圈参数研究. 岩石力学与工程学报, 2012, 31(2): 280-288 (Li Pengfei, Zhang Dingli, Zhao Yong, et al. Study of distribution law of water pressure acting on composite lining and reasonable parameters of grouting circle for subsea tunnel. *Chinese Journal of Rock Mechanics and Engineering*, 2012, 31(2): 280-288 (in Chinese))
- 19 戴新, 贺维国, 王东伟等. 深埋矿山法海底隧道排水设计探讨——以珠江口铁路隧道为例. 隧道建设, 2022, 42(4): 695-702 (Dai Xin, He Weiguo, Wang Dongwei, et al. Drainage design of a deep-buried subsea tunnel using mining method: a case study of pearl river estuary railway tunnel. *Tunnel Construction*, 2022, 42(4): 695-702 (in Chinese))
- 20 王秀英, 谭忠盛, 王梦恕等. 厦门海底隧道结构防排水原则研究. 岩石力学与工程学报, 2007, 26(S2): 3810-3815 (Wang Xiuying, Tan Zhongsheng, Wang Mengshu, et al. Study on waterproof and drainage principles of Xiamen subsea tunnel. *Chinese Journal of Rock Mechanics and Engineering*, 2007, 26(S2): 3810-3815 (in Chinese))
- 21 陈建芹, 冯晓燕, 魏怀等. 中国水下隧道数据统计. 隧道建设, 2021, 41(3): 483-516 (Chen Jianqin, Feng Xiaoyan, Wei Huai, et al. Statistics of underwater tunnels in China. *Tunnel Construction*, 2021, 41(3): 483-516 (in Chinese))
- 22 许增光, 曹成, 柴军瑞等. 断层带破碎岩体非达西渗流特性及模型研究. 岩石力学与工程学报, 2023, 42(S2): 4099-4108 (Xu Zengguang, Cao Cheng, Chai Junrui, et al. Study on non-Darcy seepage characteristic and model of the broken rock mass of fault zone. *Chinese Journal of Rock Mechanics and Engineering*, 2023, 42(S2): 4099-4108 (in Chinese))
- 23 马丹, 李樯, 张吉雄等. 断层带破碎岩体孔隙结构表征与非线性渗流特性. 煤炭学报, 2023, 48(2): 666-677 (Ma Dan, Li Qiang, Zhang Jixiong, et al. Pore structure characterization and nonlinear seepage characteristics of rock mass in fault fracture zones. *Journal of Coal Society*, 2023, 48(2): 666-677 (in Chinese))
- 24 傅鹤林, 安鹏涛, 伍毅敏等. 开挖扰动及非达西渗流对隧道涌水的影响分析. 铁道工程学报, 2022, 39(7): 80-85 (Fu Helin, An Pengtao, Wu Yimin, et al. Analysis of the influence of excavation disturbance and non-Darcy seepage on tunnel water inflow. *Journal of Railway Engineering Society*, 2022, 39(7): 80-85 (in Chinese))
- 25 孔祥言. 高等渗流力学. 合肥: 中国科学技术大学出版社, 1999 (Kong Xiangyan. Advanced Mechanics of Fluids in Porous Media.

- Hefei: USTC Press, 1999 (in Chinese))
- 26 Niu FY, Cai YC, Liao HJ, et al. Unfavorable geology and mitigation measures for water inrush hazard during subsea tunnel construction: A global review. *Water*, 2022, 14(10): 1592
- 27 肖智兴. 基于遗传算法和神经网络的水下隧道涌水量预测研究. [硕士论文]. 成都: 西南交通大学, 2011 (Xiao Zhixing. Prediction of water inflow into the underwater tunnel based on genetical gorithms and BP neutral network. [Master Thesis]. Chengdu: Southwest Jiaotong University, 2011 (in Chinese))
- 28 李术才, 李廷春, 王刚等. 单轴压缩作用下内置裂隙扩展的 CT 扫描试验. *岩石力学与工程学报*, 2007, 26(3): 484-492 (Li Shucui, Li Tingchun, Wang Gang, et al. CT real-time scanning tests on rock specimens with artificial initial crack under uniaxial conditions. *Chinese Journal of Rock Mechanics and Engineering*, 2007, 26(3): 484-492 (in Chinese))
- 29 庄楚强, 何春雄. 应用数理统计基础. 第 4 版. 广州: 华南理工大学出版社, 2013 (Zhuang Chuqiang, He Chunxiong. Fundamentals of Applied Mathematical Statistics. 4th Edition. Guangzhou: South China University of Technology Press, 2013 (in Chinese))
- 30 Katibeh H, Aalianvari A. Development of a new method for tunnel site rating from groundwater hazard point of view. *Journal of Applied Sciences*, 2009, 9(8): 1496-1502
- 31 铁路隧道设计规范: TB 10003—2016. 北京: 中国铁道出版社, 2016 (Code for Design of Railway Tunnel: TB 10003—2016. Beijing: China Railway Publishing House, 2016 (in Chinese))
- 32 关宝树. 漫谈矿山法隧道技术第十四讲——隧道涌水及其控制方法. *隧道建设*, 2017, 37(1): 1-10 (Guan Baoshu. Tunneling by mining method, Lecture XIV: Tunnel water inrush and its countermeasures. *Tunnel Construction*, 2017, 37(1): 1-10 (in Chinese))
- 33 Aalianvari A, Katibeh H, Mostafa S. Application of fuzzy Delphi AHP method for the estimation and classification of Ghomrud tunnel from groundwater flow hazard. *Arabian Journal of Geosciences*, 2012, 5(2): 275-284
- 34 Myles AJ, Feudale RN, Yang L, et al. An introduction to decision tree modeling. *Journal of Chemometrics*, 2004, 18(6): 275-285
- 35 Quinlan JR. C4.5: Programs for Machine Learning. USA: Elsevier, 2014
- 36 郑力嘉, 宋冰. 决策树分类算法的预剪枝与优化. 自动化仪表, 2023, 44(5): 56-62 (Zheng Lijia, Song Bing. Pre-pruning and optimization of decision tree classification algorithm. *Process Automation Instruction*, 2023, 44(5): 56-62 (in Chinese))
- 37 Raileanu LE, Stoffel K. Theoretical comparison between the gini index and information gain criteria. *Annals of Mathematics and Artificial Intelligence*, 2004, 41(1): 77-93